environments

MDPI

Article

TENORM Industries and Alpha Spectrometry: Spectra Deconvolution

Concepción Olondo *, Asier Gamarra, Raquel Idoeta and Margarita Herranz

Energy Engineering Department, University of the Basque Country, EHU 1 Ingeniero Torres Quevedo Square, 48013 Bilbao, Spain; agamarra007@ikasle.ehu.eus (A.G.); raquel.idoeta@ehu.eus (R.I.); m.herranz@ehu.eus (M.H.)
* Correspondence: kontxi.olondo@ehu.eus

Abstract

Alpha spectrometry is a useful method for measuring alpha emitters in all types of samples and for all types of radioisotopes, both artificial and natural. The high activity concentration of TENORM industries' by-products and their management are of great concern; however, due to the high activity and the complex matrixes of these types of wastes, there are overlaps between peaks and an acute activity determination can require a high consumption of time and material. To diminish it and obtain a proper activity evaluation, spectra deconvolution has been carried out using a genetic algorithm to fit the selected function to experimental data. This algorithm uses the analyst's visualization of the observed experimental spectrum as a reference and adapts the fitting parameters to the observed peak. This gives the algorithm great capacity to adapt to different spectra obtained experimentally. The results of its application to different TENORM samples have been very satisfactory, including complicated multi-energetic alpha emitters such as Th-229.

Keywords: TENORM; waste management; alpha spectrometry; deconvolution

1. Introduction

Naturally Occurring Radioactive Material (NORM) is defined as material that contains any of the primordial radionuclides or radioactive elements as they occur in nature, such as those of thorium, actinium and uranium decay series products, including radon and potassium, and are not disturbed because of human activities. Technologically Enhanced Naturally Occurring Radioactive Material (TENORM) is defined as material that has been concentrated or exposed to the accessible environment because of human industrial activities. In fact, these industrial activities concentrate or further alter the radiological, physical, and chemical properties of the radioactive material when they are processed or disturbed during industrial activities, increasing because of it human and/or environmental radioactive exposure.

The major industries that generate TENORM wastes and residuals are mineral extraction, including those of Rare Earth; energy production, such as gas and petroleum extraction; and fertilizer production. The final treatment of their waste products depends on their radiological characterization. Because TENORM wastes are generated by many industries in varying amounts and occur in a wide variety of products, the management of TENORM is a complex issue [1].

These radioactive wastes produce different types of radiation emissions (alpha, beta and gamma) and usually are of high activity concentration. Due to the risk that exposure to this radiation entails, attention has been focused on the environmental and health

Check for updates

Academic Editors: Sergio Ulgiati and Javier R. Viguri

Received: 27 December 2025
Revised: 11 February 2026
Accepted: 14 February 2026
Published: 18 February 2026

Copyright: © 2026 by the authors. Licensee MDPI, Basel, Switzerland. This article is an open access article distributed under the terms and conditions of the Creative Commons Attribution (CC BY) license.

effects of them and so on their final management [2,3]. The waste materials of TENORM industries include large amounts of production waters and solid wastes. The first one can be discharged into the aquatic systems only after being very diluted; the management of solid waste is limited. These waste materials include alpha emitters such as Ra-226, U-238, U-235, U-234, Th-230, Th-232 and Po-210, known for their high radiotoxicity [3].

Alpha-emitting radioisotopes must be analyzed using alpha spectrometry. Prior sample preparation is required for this. After adding a tracer to evaluate the yield of the subsequent radiochemical separation procedure, the radioisotopes of interest are extracted from the sample. They are then electrodeposited onto a stainless steel planchet to form an alpha source. This alpha source is then placed in front of the detector. Due to its low background, alpha spectrometry is a useful method for analyzing alpha-emitting radionuclides, particularly when measuring environmental samples. The obtained source must be very thin and homogeneous to achieve the highest possible energy resolution and thus the narrowest possible peak [4].

However, the complexity of TENORM matrices further complicates the radiochemical procedures that must be implemented, increasing the matrix effects and making it difficult to obtain a thin, homogeneous alpha source. This widens the spectrum peaks and diminishes the energy resolution, resulting in nearby peaks overlapping. Similarly, the high activity concentration of these types of samples increases the peak overlap by increasing the size and width of the recorded peaks. Therefore, alpha spectrometry faces challenges when analyzing these types of samples, as it must obtain extremely thin and uniform alpha sources after performing complex radiochemical separations of the samples in order to achieve the best possible resolution and perform correct peak analysis despite spectral interferences from overlapping peaks [5]. Recoil nuclei contaminate alpha spectrometry detectors, a risk that rises with high activity samples; this laboratory uses a thin film to avoid this contamination [6].

When performing an alpha spectrometry measurement, parameters such as the treated sample mass selection, distance between the detector and counting time [5] must be adjusted. To reduce the peak overlap, the amount of sample to be treated must be nearly massless and the distance between the detector and the alpha source must be increased. The counting time must also be limited.

On the one hand, due to the high concentrations of activity that TENORM samples can have, a priori unknown, the establishment of the mass, the counting time and the appropriate source detector distance for this determination is not trivial.

Despite analyzing a very small amount of mass, it is sometimes necessary to adjust the measurement parameters to achieve a good spectrum. This adjustment is difficult to achieve since, despite the nearly massless samples used, it could have high activity. Thus, to avoid overlap between the unknown peaks and the tracer peak, it is necessary to control the measurement time and/or the distance between the source and detector. However, despite this control, an adequate spectrum cannot always be obtained, necessitating the repetition of the analysis with a smaller mass and the readjustment of the distance and time, which is time-consuming and involves the use of more material.

On the other hand, TENORM waste materials have very complicated matrices, which increases the presence of impurities in the thin source to be measured, even when appropriate radiochemical separation processes are performed. This fact increases the alpha particle self-absorption and energy loss, resulting in an increase in the tails of the spectrum peaks and, consequently, the likelihood of overlapping.

To reduce the repetition of samples and the sequence of different measurements, it has been decided to deconvolve the spectra to determine the activity despite the overlaps.

To carry this out, it is necessary to determine the mathematical expression that best fits with the peaks of the spectrum obtained using PIPS detectors, the most common detector used by laboratories to perform alpha spectrometry [5,7]. Various peak models have been proposed in the past [8–12], with [12] being the most successful analytical one. The spectra of alpha monoenergetic particles shows an asymmetric shape and can be expressed as the convolution of a Gaussian with exponential probability density functions [12–16]. Other authors had tried to deconvolve alpha spectra based on the mention function [17,18], observing some important inconsistencies [19]. The models used to simulate alpha spectrum peaks have evolved as computer resources have done; some authors have used artificial neuronal networks [20] to analyze alpha spectra, and more recently, MCNP [7] and deep learning machines together with MCNP to simulate the spectra used to train the machine [19]. The goal of the mentioned studies and, thus, of the model used is different from that of ours as they pretend to identify and quantify the radioisotopes of the spectrum or simulate the counting efficiency and energy resolution. All of them conclude that the analysis of alpha spectra is still a challenging issue.

Among the available methods, some can only provide results for the type of peaks used when building the model, very clear and defined peaks, which defeats the purpose of obtaining results from more complex experimental data [20]. Others obtain the fit using multiple function approximations for each emission peak, but the excessive degrees of freedom employed can approximate all variations without discriminating against them and little peak interferences can be assumed to be part of single one [16].

To develop a useful tool for this application, a simplified version that represents the shape of an emission peak is preferred, where each emission peak is completely represented by a single approximation. To select the mathematical expression that better fits the detector's registered alpha peaks, different statistical distributions have been fit to the same spectrum obtained from traced distilled water sample. This has been performed using a single approximation applying the same algorithm, Excel Solver's Evolutionary method. This gives the opportunity to compare experimental data against the ideal theoretical distribution. After selecting the proper equation, TENORM samples' spectra have been analyzed. The fits have been accomplished by analyzing only the region where the overlapping occurs, both by limiting the approximation to the isolated region of the peak not disturbed by surrounding peaks and by including many approximations where multiple emissions are involved. This permits adequately approximating any type of peak, monoenergetic or multi-energetics, since all emissions are accounted for, without including other disturbances.

Unlike other methods [7,19], this only requires the information of the sought peaks, emission intensities and energies to be able to differentiate interfering signals, and it does not require the use of any number of spectra for training the algorithm nor to carry out its calibration to adapt the approximation to the region of interest. This approach allows the procedure to validate results using internal parameters of each approximation, derived from actual physical evidence: energy shift correlation and resolution coherence. Human uncertainty serves as a delimiter for the maximum variation of the results.

In this work, the goal of the algorithm used to fit the peaks obtained in alpha spectrometry is to evaluate in a proper way the number of counts that belong to each radioisotope peak when peak overlap occurs to correctly evaluate the activity concentration of the radioisotopes of interest. This fitting is controlled by the analyst responsible for reporting the activity concentration of the analyzed sample, despite the unfavorable conditions to perform a classical analysis, as happens during overlaps because of the high activity of the sample or the complexity of the matrix. In any case, the algorithm will not be responsible for identifying the radioisotopes that appear in a spectrum: the first parameters to include

in the algorithm will be established by the analyst and not by a code trained with very defined peaks, which is rarely obtained when complex matrixes are under study. The code will then iterate those parameters in search of an optimal fit within the established bounds.

The acceptable limit for the error has been set to be the same as the uncertainty associated with the analyst (2.5%), where higher values are considered to introduce a higher error than without the use of the approximation. Additionally, it has been observed that, for a given spectrum, peaks behave in a similar fashion in spite of the type of matrix or applied radiochemical procedures. This signifies that parameters reflecting the resolution (later dubbed "Shape Factors") must not vary excessively, which has been experimentally set at a maximum of 20%. Additionally, energy loss behavior demonstrates that lower emission energies are more prone to suffer a higher energy shift, which forces peaks on the left (low energies) to have a higher energy shift than their peers on the right (higher energies).

2. Materials and Methods

2.1. Instrumentation

The alpha spectra used to carry out the study have been registered in the Alpha Analyst Integrated Alpha Spectrometer of Mirion Technologies (Atlanta, GA, USA), equipped with a Passivated Implanted Planar Silicon (PIPS) detector of 450 mm^2, with an efficiency of about 25% at 5 mm detector–source distance and 5.8×10^{-5} cps background.

The energy and efficiency calibration of the detector is established using a standard electroplated calibration source of U-233, Pu-239 and Am-241 of 96.5 Bq. The vacuum of the detector chamber is lower than 0.3 mm Hg.

GENIE 2000 3.1. Alpha Analysis Software is used to record the experimental spectra.

2.2. Materials

The spectra to be fitted with the mathematical expression come from wastes and products of TENORM industries that, after performing the appropriate radiochemical separation, have been electrodeposited on a steel and nickel disk. All of them have an important activity of one of the radioisotopes under study: that of thorium (Th-230) is a thorium fabric, that of uranium (U-238, U-234 and U-235) comes from uranium mining and that of polonium comes from oil and gas production industry.

Each one of these samples has been radiochemically treated to obtain a thin alpha source.

The activity concentration of these samples is calculated following this equation:

$$A = (r_g - r_0)/(m \cdot R) \quad (1)$$

where

- A: the activity concentration of the sample [Bq/kg or Bq/m^3];
- r_g: the gross count rate in the analyzing radioisotope spectral ROI (region of interest) of the spectrum [s^{-1}];
- $r_{0:}$ the gross count rate in the analyzing radioisotope spectral ROI (region of interest) of the background spectrum [s^{-1}], the same ROI of the analyzing spectrum;
- m: the mass of the sample used to perform the analysis [kg or m^3];
- R: the total yield of the radiochemistry and measurement process [-].

The total yield is calculated as follows:

$$R = (r_{At,g} - r_{At,0})/A_t \quad (2)$$

where

- $r_{At,g}$: the gross count rate observed in the tracer radioisotope spectral ROI of the sample spectrum [s^{-1}];
- $r_{At,0}$: that of the same ROI's of the background spectrum [s^{-1}];
- A_t: the activity of the tracer added to the sample [s^{-1}] when the radiochemical separation process is carried out.

The goal of this work is to properly determine the number of counts that effectively belong to each of the isotopes observed in the spectrum when peak overlapping occurs, usually that of the tracer and the radioisotope of interest, as they are necessary to correctly evaluate the gross rate of the tracer and the isotope and, thus, to report a proper activity concentration.

To select the mathematical expression that could fit better to the peaks recorded in the spectrum, distilled water samples have been traced with Th-229, U-232 and Po-209, the tracers added to the mentioned TENORM samples.

2.3. Data Processing

The data processing involves the following steps:

- Data acquisition
- Parameter presetting
- Algorithm execution
- Result processing

2.3.1. Data Acquisition

The spectrometry result values must be inputted. To do this, a text-file-compatible data document is needed, where both the counts and their associated energy are provided. In this case, the Excel document searches for a matching ".TKA" document, generated by the Genie 2000 3.1 Alpha Analysis Software, which holds the results from each energy channel in a list, substituting the first two with the current measure time and the maximum measure time.

To be able to relate the channel number to their energy values, the energy calibration curve (typically, in the form of a first degree polynomial) must be provided.

The spectrometry results are then pasted into the appropriate field, and the first two cells are substituted by zero, effectively erasing the time values, as they do not contain counts and their energy values are out of the region of interest (ROI). Inputting the energy calibration curve's exponents in the preset cells allows for the channel number to be converted into energy. This way, the Excel file can operate with the natural numbers of the data channel numbers (one per row), while the graphs and results can provide information referencing the corresponding energy.

2.3.2. Parameter Presetting

It is necessary to set constraints on the region where the algorithm is going to be fitted to avoid the interference of irrelevant data. With the visual aid of the generated graphs, the analyst can input the ROI minimum and maximum values to set boundaries. These graphs can also help visualize the whole process.

For each iteration variable, the algorithm requires constraints be set to be able to perform the iterations. These values will constitute the upper and lower bounds of the variables involved in the function and can be set according to different criteria:

- Radioisotope behavior: emission ratios for activity, emission energy difference, etc.
- Experimental experience: radioisotopes identification, spectrum distortion, etc.
- Observation of the spectrum: total activity, etc.

Given that the chosen function's parameter's influence is known, the analyst is usually able to approximate the spectrum by manually altering the values to narrow down the initial converging steps of the iteration process. This step is optional but saves computational cost and allows us to set the iteration value's boundaries more intuitively, without resorting to trial and error.

For a simulation to be deemed successful, none of the bounds must have been reached unless some data unrelated to the spectrometry justifies it. Reaching variable bounds limits said variable's values, which usually means the optimal value lays beyond the set limit.

It is common and recommended to change the variable bounds between algorithm executions, to set the boundaries centered around the current value and to give the algorithm the chance of exploring more relevant values. With the intention of increasing the accuracy of the results, it is suggested to reduce the range of possible values by setting the limits closer to the current values once the algorithm has been run a few times and the values do not show relevant changes.

It is possible to approximate more than one peak at a time. Depending on the circumstances, it might be necessary to use multiple peaks for a proper characterization of the spectrum. The two most notable cases are the overlapping emissions from different radionuclides and multi-energetic emissions of a single radionuclide.

2.3.3. Algorithm Execution

After everything has been prepared, the algorithm is run. With replicability in mind, the initial ad hoc algorithms have been discarded in favor of a standard one that would allow for a function comparison without external factors. Additionally, due to the multivariable and nonlinear nature of the problem, algorithms with some kind of pseudo randomness are preferred, since it is not possible to guarantee optimal results for local relative extremes for the error.

The Evolutionary resolution method in Excel Solver was chosen, which employs a Genetic Algorithm (GA). GAs are a metaheuristic type of algorithms inspired by natural selection. These GAs create random values (or "generations") around the current values and then check their fitness level according to the optimization criteria. The unfit values are rejected, while the better-suited values act as "parents" and become the new "current values" that will serve as a basis for the next generation.

In our specific situation, the optimization criteria entails the minimization of the error. The algorithm first creates the random values within the boundaries from the current ones, then selects the combination that minimizes the value of the error. From these values, new generations are formed. To avoid limiting the available results by getting stuck in local optima or losing diversity in the population, Solver also introduces random values in each generation.

Figure 1 shows the work process of the Evolutionary Algorithm.

This algorithm would fit the selected mathematical function to experimental spectra following an iterative process. The best result is always kept and, when the resulting error does not reduce any further during a set amount of time, the iterations are finished. For optimal results, it is recommended to adjust the boundaries after each run until the result after two consecutive runs is the same and the boundaries are around 95% and 105% of the final value.

For each energy channel, the selected formula is used with the parameters provided by the algorithm. In this manner, a new estimate for the counts at each channel is obtained. Now, the error between the estimated and the experimental values can be calculated. The addition of all the errors in the region of approximation constitutes the value the Evolutionary method aims to minimize.

The least squared mean (LSM) error method has been selected for the characterization of the fitting error.

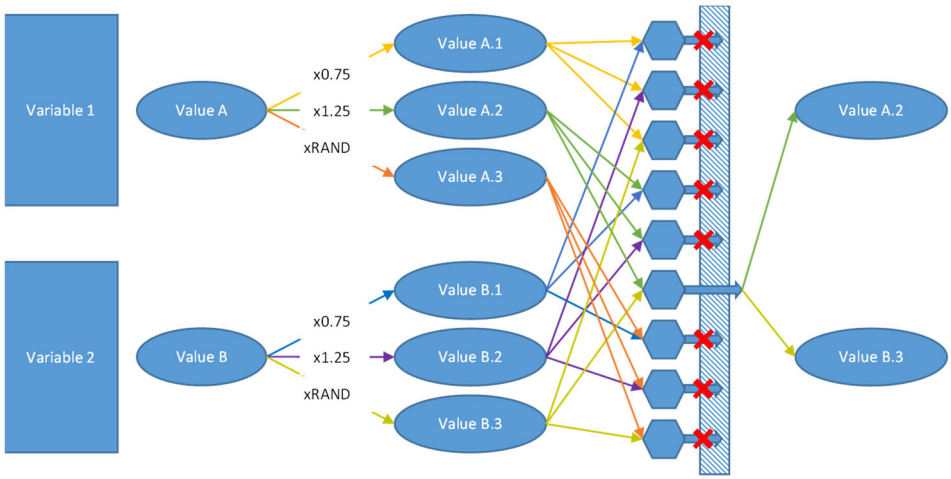


Figure 1. Work process of the Evolutionary Algorithm.

2.3.4. Result Processing

Once the approximation cannot be realistically improved, a visual inspection must confirm that the spectrum is properly fitted by the approximation. The data are then compared in a new table that helps perform a comparison depending on the intent of the user. Two graphs support the results for a better understanding.

Since the functions themselves span across any value for the abscissas (where the energy is represented), the region of the relevant values must be provided to obtain the desired results. This new region is usually related, but not necessarily limited, to the ROI and is usually defined as the region wherein all the values for the function are over 0.5, with the edges being the ones in which the values are under 0.5.

2.4. Function Fitting

Before tackling more complex spectra, we will resort to single peaks that allow us to choose the optimal function for approximating alpha spectra. The peaks of water samples traced with Th-229, U-232 and Po-209 have been fitted using selected functions. The monoenergetic alpha emitter Po-209 has been the first peak to be fitted. Following this, the selected function is applied to deconvolve the Po-209 and Po-210 peaks overlapping and, finally, the other tracers' peaks, U-232 and Th-229, multi-energetic emitters, are fitted. As mentioned, the error associated with the fit is calculated by means of the least squared mean error method and the criteria that each fit have to fulfill are that the difference between the number of counts recorded in the selected ROI of the peak and that provided by the fit must be lower than the uncertainty associated with the analysis performed by the analyst when carrying out the spectrum analysis: 2.5%.

Following this, TENORM samples are fitted by performing the deconvolution of U-235 and U-234 and Th-230 and Th-229.

3. Results and Discussion

3.1. Function Fitting

First, the function that best fits the peaks recorded in the spectrum was selected. To do this, several statistical distributions were tested, such as Gamma, Log-Normal and Weibull, to fit the alpha emissions. These distributions were used together with the convolution of multiple exponential functions for the low-energy tail with a Gaussian distribution, as

described in [12–16]. For a complete characterization of the spectrum, the authors [16] suggest a weighted approximation with different characteristic lengths of the function to replicate a complete peak.

In contrast, this work aims to provide accurate activity concentration results when the spectrum to be analyzed is complex, as is the case when peaks overlap. Therefore, a simpler and more focused characterization is preferred, and the algorithm is only applied in the spectrum ROI determined by the analyst. To discriminate random errors inherent in the measurement statistics, a single function per peak is used, thus avoiding an adjustment that would also include these errors. Due to the distinctive feature of using the complementary error function, this method has been named the "Erfc Approach".

Figure 2 and Table 1 show the results of fitting Po-209 with the mentioned statistical distributions using the GA. Figure 2 shows the fit of the mathematical expressions to the peak of Po-209 registered in the spectrum, whilst Table 1 shows the number of counts obtained by each fit, the number of counts registered under the peak and the difference between both numbers expressed as the error committed.

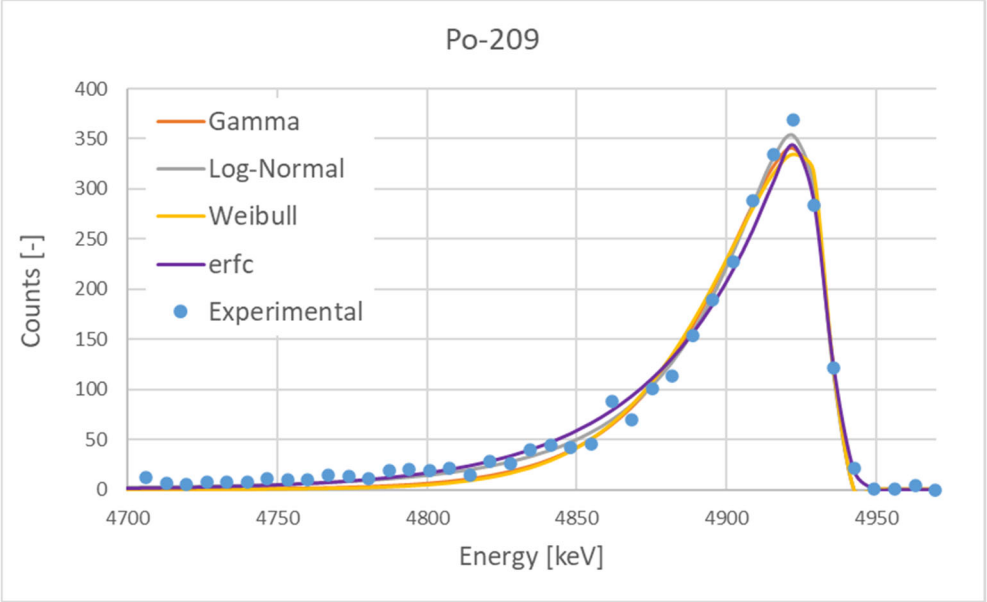


Figure 2. Selected distributions fitting to the Po-209 spectrum.

Table 1. Counts estimated by each function in the selected region and the error committed.

Distribution	Experimental Counts [-]	Estimated Counts [-]	Count Difference [-]	Relative Error [%]
Gamma	2867	2571.41	−295.588	−10.31
Log-Normal	2867	2720.05	−146.954	−5.13
Weibull	2867	2561.66	−305.34	−10.65
Erfc	2867	2732.26	−134.741	−4.70

In view of the results and supporting the existing literature [16], the Erfc approach has proven to be the most accurate.

$$f(u-\mu,\ \sigma,\ \tau) = A/(2\tau)\cdot \exp\left[(u-\mu)/\tau + \sigma^2/\left(2\tau^2\right)\right]\cdot \operatorname{erfc}\left[1/\sqrt{2}\cdot(u-\mu)/\sigma + \sigma/\tau\right] \quad (3)$$

This function is an exponentially modified Gaussian distribution. Each parameter has been empirically tested to influence the following part of the distribution:

- A: area or activity, direct effect on total "height" of the peak;
- σ: standard deviation of the Gaussian (controls peak width), exchanges peak height for slope steepness on both sides;
- τ: tailing parameter (controls low energy peak width), also exchanges height but mostly affecting the left slope; and
- μ: energy displacement, changes the value the peak is centered around.

When dealing with complex spectra, two cases are of relevance: peak overlap and multi-energetic emissions.

3.1.1. Peak Overlap

When the matrix of the sample increases the effects of the distortions of the emissions or the activity is a lot higher than expected, it is possible to find some counts of a radioisotope in the emission energy range of another, making their ROIs overlap. This prevents a simple addition of the counts in their respective areas from being performed, since the asymmetrical distribution makes it impossible to accurately pinpoint the counts intruding into each peak area.

To address this issue, instead of the single function used before, two are used for the approximation. Now, the ROI encompasses both peaks, while each function tries to approximate one of them. The results are shown in Figure 3 and fulfill the established criteria: their error must not exceed the uncertainty associated with the work of the analyst (2.5%).

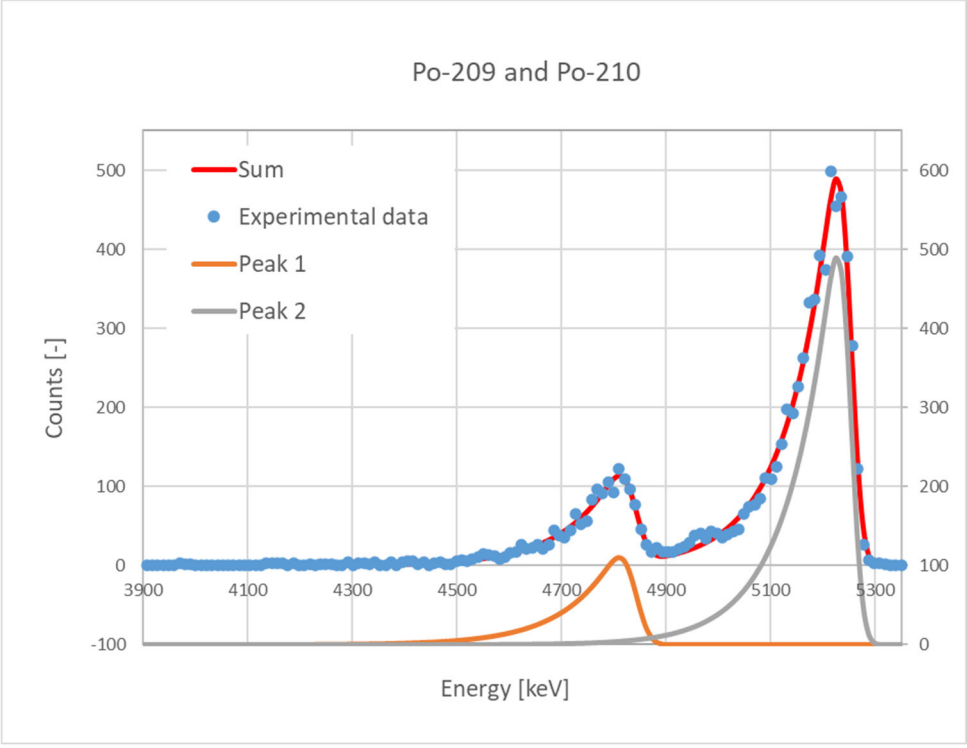


Figure 3. Polonium spectrometry approximation by two erfc-based distributions.

There are two ways to calculate the resulting counts: either subtracting the other peak from the total spectrum ("cleaned" values) or using the function of that peak (estimated values, "Peak X" function). For the sake of verification, both are shown in Table 2.

Table 2. Results of the polonium spectrometry approximation by two erfc-based distributions.

Study Region	Channel [-]	Energy [keV]	Cleaned Counts [-]	Estimated Counts [-]	Count Difference [-]	Error [%]
Po-209	392 454	4259.96 4903.52	1587.41	1548.43	−38.99 [1]	−2.46 [1]
Po-210	427 493	4623.26 5308.34	5939.05	5935.25	−3.81 [1]	−0.06 [1]
All spectrum	392 493	4259.96 5308.34	7517	7487.35	−29.65 [2]	−0.39 [2]

[1] Difference and error between different approaches, not to be assumed as an actual experimental error. [2] Values obtained directly from actual experimental data.

The values of the peaks' parameters are summarized in Table 3.

Table 3. Parameters of the two functions employed in the polonium spectrometry approximation.

Distribution	A	σ	τ	μ
Peak 1	16,412.44	20.72	99.01	4842.28
Peak 2	62,682.84	17.19	85.69	5253.89

Studying the parameters of each function, the relative similarity of the "shape factors" sigma and tau is apparent. While it is true that many factors affect a spectrum's resolution, within each spectrum the same variables apply (except for the emission energy). However, when the emissions can be said to take place at very similar energy, assuming both shape factors are the same for the two peaks seems plausible. The results show that, for the cases under study (<500 keV difference between peak emissions), the values differed by at most 20% from each other. This value seems like a good quality control test and has been established as such.

Testing showed that, while the computational speed increased due to the reduction of the variable amount, some distortion took place when using the same shape factors in both peaks' functions. The peak with the most activity overrode the smaller one's shape factors, forcing the small one to disregard its own shape and mimic that of the big one, resulting in a significant error increase. Check Tables 4 and 5 for the results and values, respectively.

Table 4. Results of the polonium spectrometry approximation by two Erfc-based distributions with shape factor equality.

Study Region	Channel [-]	Energy [keV]	Cleaned Counts [-]	Estimated Counts [-]	Count Difference [-]	Error [%]
Po-209	398 453	4322.24 4893.14	1566.08	1434.18	−131.90 [1]	−8.422 [1]
Po-210	426 493	4612.88 5308.34	6005.53	5965.10	−40.43 [1]	−0.673 [1]
All spectrum	398 493	4322.24 5308.34	7506	7402.74	−103.26 [2]	−1.376 [2]

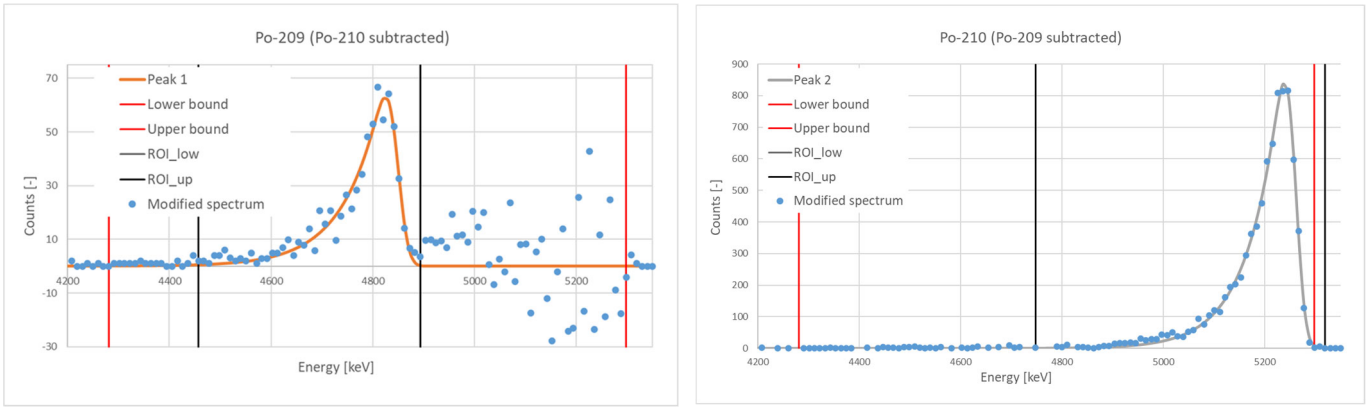
[1] Difference and error between different approaches, not to be assumed as an actual experimental error. [2] Values obtained directly from actual experimental data.

Table 5. Parameters of the two functions employed in the polonium spectrometry approximation by the shape factor equality.

Distribution	A	σ	τ	μ
Peak 1	15,171.55	17.27	86.66	4839.82
Peak 2	62,982.81	17.27	86.66	5254.03

Comparing both tables, Tables 4 and 5, it is obvious how the shape factors for the second peak remain practically constant (changes of 0.5% and 1%), while the first, which presents a huge error increase, changes a lot more (17% and 13%). Taking this fact into account, it is not recommended to use this last approach unless the emission energies are close enough to warrant a negligible difference in the shape factors and the potential shape factor dissimilarity distorts the approximation.

Now, although there is an inevitable uncertainty factor included, it is possible to perform an analysis of each peak independently, without restricting the ROI to the isolated region. In the following figures (Figure 4a,b), the experimental data are shown together with the subtraction of the "interfering" peak. Since the counts are placed around the function, the approximation is deemed successful. It is apparent, however, that the function cannot perfectly match the spectrum. This is proof that there are unavoidable error sources present in the experimental data itself (background, statistical, etc.), which caps the error reduction that the function can reach.



(**a**) (**b**)

Figure 4. Isolated representation of the two approximated polonium peaks, showing the subtraction of the interference and the approximating function: (**a**) Po-209 approximation; and (**b**) Po-210 approximation.

When an overlap happens, only an approximation is possible, since the values intrude into each other's ROI disproportionately. If the overlap is not significant, the effect is negligible. In the example above (Table 6), the usage of the experimental data yields an activity 2% lower than its isolated counterpart (average values of the counts in Table 2), while the added errors almost reach 2%. However, due to the calculations involved, the calculated activity exponentially varies as more counts overestimate one peak while underestimating the other.

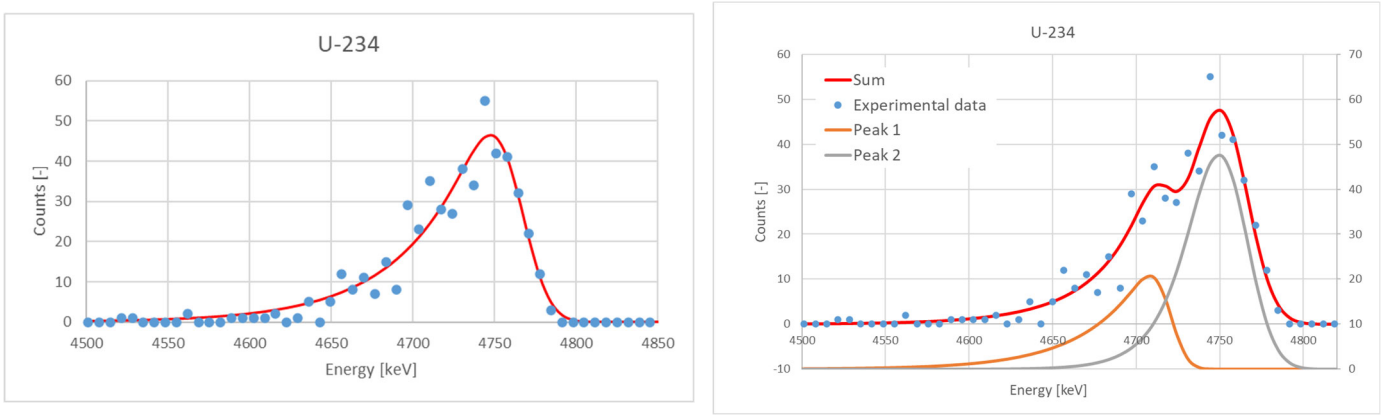
Using a peak separation method resolves this issue in exchange for an increase in uncertainty. Since many factors influence the measurement, it is not possible to nullify the error. However, it is possible to obtain a statistically representative distribution to characterize the spectrum, which avoids the disturbance of the overlap.

Table 6. Results of the isolated peaks of the polonium spectrometry.

Study Region	Channel [-]	Energy [keV]	Counts [-]	Count Difference [-]	Error [%]
Experimental Po-209	410 451	4446.80 4872.38	1589	−21	−1.32
Isolated Po-209	392 454	4259.96 4903.52	1568		
Experimental Po-210	451 495	4872.38 5329.10	5898	39	0.66
Isolated Po-210	427 493	4623.26 5308.34	5937		

3.1.2. Multi-Energetic Emissions: Uranium and Thorium Spectrometry Approximation

When encountering multi-energetic emissions, it is necessary to know the emissions of the isotope under study to accurately differentiate peaks belonging to other isotopes. However, a single function approximation cannot appropriately reflect the real distribution, even when the count difference is promising, as can be seen in Figure 5.



(**a**) (**b**)

Figure 5. Approximation of a U-234 spectrum: (**a**) single peak approach; and (**b**) double peak approach.

Checking Figure 5, the double peak approach fits the function better (LSMs of 614 vs. 463, respectively). What is more, the parameters involved suggest some mathematical overfit is in place. Table 7 shows the parameters of the two functions employed in the U-234 spectrometry approximation

Table 7. Parameters of the two functions employed in the U-234 spectrometry approximation.

Distribution	A	σ	τ	μ
Peak 1	1156.06	8.09	36.13	4720.15
Peak 2	3047.78	14.19	17.25	4765.31

The vast difference between the sigma and tau factors suggests the physical meaning behind the shape factors has been lost. The extreme closeness of the peaks hinders the algorithm's capacity to shape each peak properly, even when experience tells us that they should be almost identical due to their energy closeness. To make sure this does not happen, we force these parameters to share the same values.

Fortunately, the activity ratio among different emissions is known, which allows us to further reduce the number of variables. Below, the three most intense emissions of U-234 are shown with their corresponding emission energy [21].

- 4604.9 keV: 0.24%;
- 4723.8 keV: 27.50%;
- 4776.1 keV: 72.50%.

The new restriction increases the LSM slightly (from 463 to 507), but the data obtained are more realistic and the calculus is more robust (see Figure 6). Table 8 shows the values of the parameters of the three functions employed in the U-234 spectrometry approximation with shape factor equality and Table 9 shows the U-234 spectrometry approximations, with and without shape factor equality.

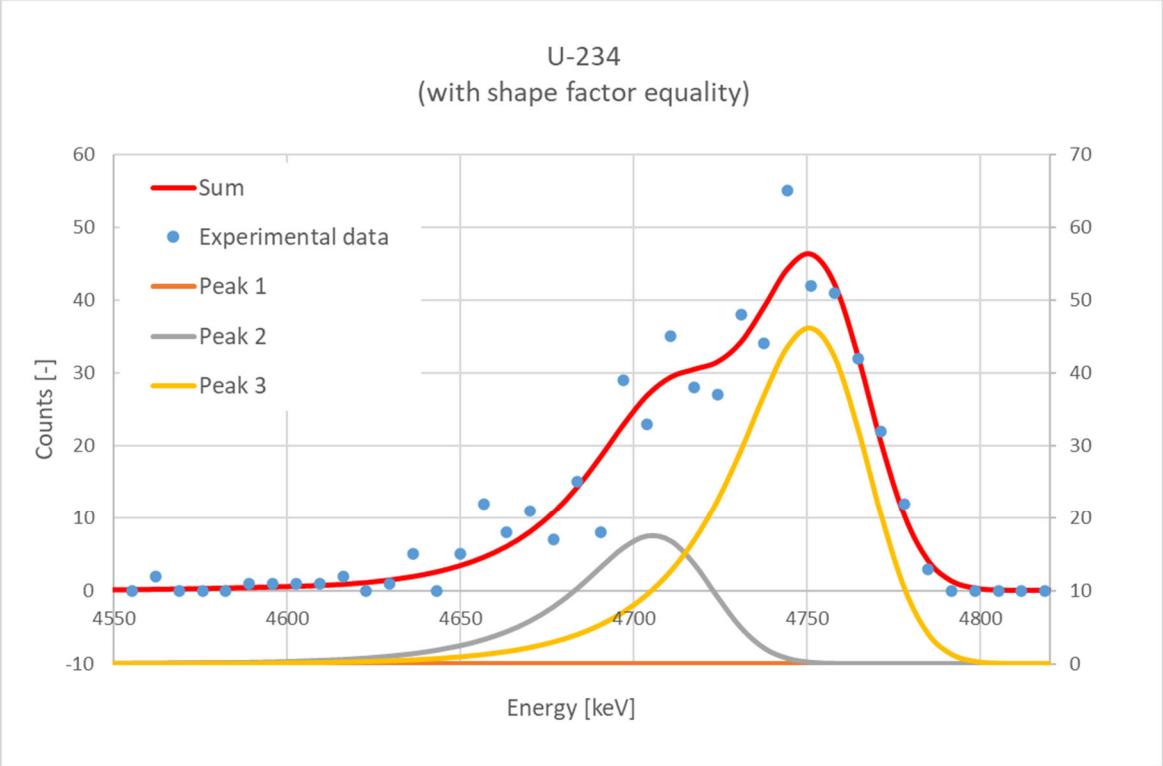


Figure 6. U-234 spectrometry approximation by two erfc-based distributions with shape factor equality.

Table 8. Parameters of the three functions employed in the U-234 spectrometry approximation with shape factor equality.

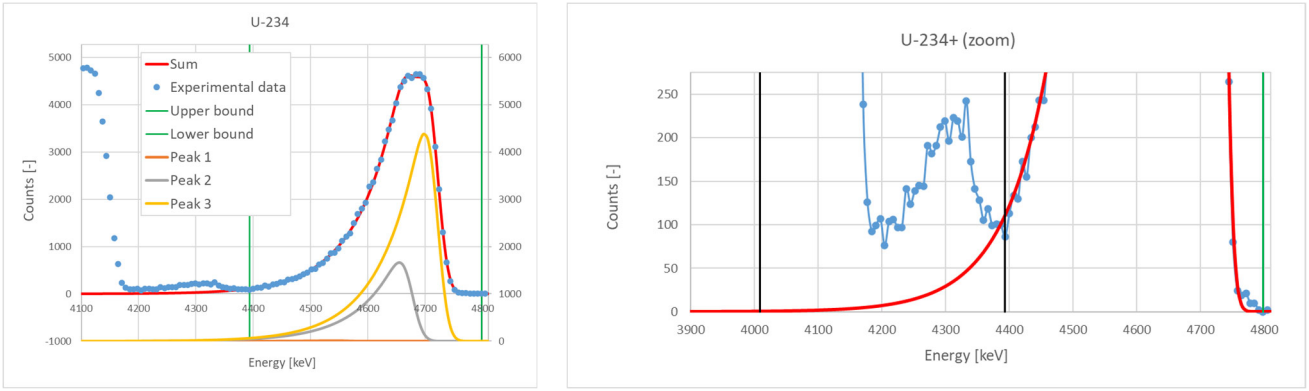
Distribution	A	σ	τ	μ
Peak 1	9.08	13.08	23.32	4605.00
Peak 2	1040.67	13.08	23.32	4721.16
Peak 3	2743.59	13.08	23.32	4766.27

Now, since we can determine the shape of the peak associated with an isotope accurately, it is possible to obtain good predictions that can be dissociated from local disturbances. Even if an approximation encompassing both emissions would be very complicated, sufficient "independent" data can allow us to create a solid prediction even outside the chosen ROI.

Table 9. Result comparison of the U-234 spectrometry approximations, with and without shape factor equality.

Study Region	Channel [-]	Energy [keV]	Experimental Counts [-]	Estimated Counts [-]	Count Difference [-]	Error [%]
U-234	346 381	4562.15 4798.37	501	506.85	5.85	1.168
U-234 (equal shape factors)	351 381	4595.90 4798.37	498	491.56	−6.44	−1.293

In the following figure, Figure 7, the U-235 and U-238 emissions overshadow the low energy tail of the U-234 distribution due to its high activity. In Figure 7, from the left side to the right, it can be seen that the peaks overlap: U-238 with U-235 and this latter with U-234.



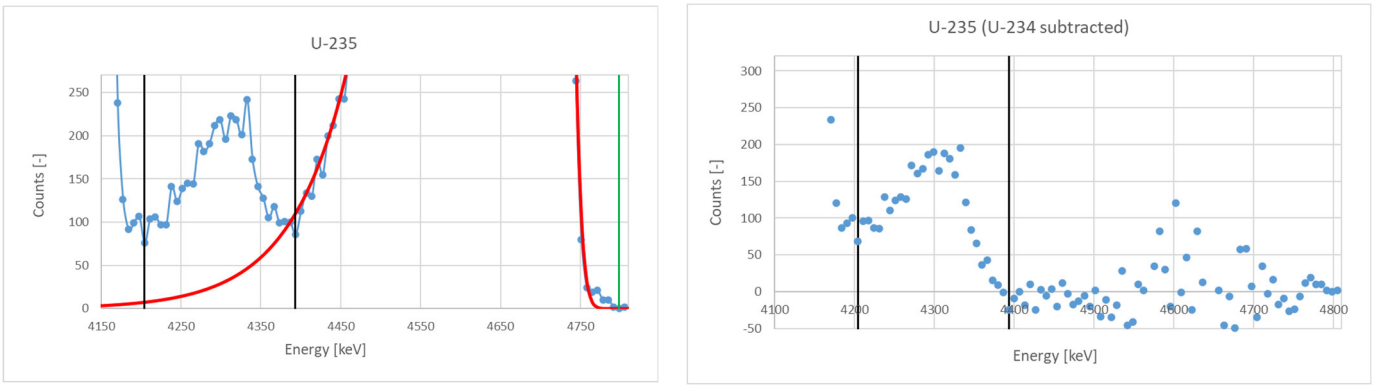
(**a**) (**b**)

Figure 7. Overlapping U-234 spectrometry approximation: (**a**) selection of the region of approximation; and (**b**) extended non-null region of U-234 (defined until counts < 0.5) overlapped with U-238 and U-235.

While we cannot calculate the missing counts of U-234, its undisturbed portion (with a 0.15% error between the experimental and approximated counts) is enough to create a very good approximation that allows us to estimate the missing 1233 counts within the region delimited using vertical black lines, that of U-235. Not only this, but it is now possible to deduct this amount from the spectrum of U-235 to erase its disturbing effect (Figure 8). If U-235 had been measured as it is, it would have been overestimated by more than a third of its real value.

The results of the isolated peaks of the uranium spectrometry are shown in Table 10.

The complex emission distribution of U-235 make it seriously difficult performing an approximation. Additionally, its relatively low activity makes it very susceptible to background noise influences. Fortunately, having a proper characterization of the neighboring peaks permits removal of their effects from the spectrum, making an accurate analysis possible.



(**a**) (**b**)

Figure 8. Overlapping U-235 spectrometry approximation: (**a**) obtained experimental spectrum; and (**b**) isolated representation of U-235 after subtracting the counts of the U-234 approximation.

Table 10. Estimated U-234 over estimated U-235 count.

Study Region	Channel [-]	Energy [keV]	Experimental Counts [-]	U-234Estimated Counts [-]	Count Difference (Isolated U-235) [-]	Error [%]
U-235	293 321	4204.46 4393.43	4300	1134.48	3165.52	35.84

As the number of variables increases, the approximation becomes more complex and more simplifications must be assumed. These simplifications often result in some accuracy loss but increase the precision of the approximation significantly, since they avoid potential overfit issues. One such example is the case of Th-229, which is often used as a tracer in thorium spectrometry but presents a complex emission distribution (much like U-235) and is close enough to the emission region of Th-230 to constitute a potential overlapping issue.

Being a tracer, not only is it significant to obtain the separated data for the characterization of Th-230 but also for the whole spectrum. That is the reason why it has been decided to tackle the issue. It is important to set criteria that discriminate unsuccessful approximations from the rest.

It is known that Th-229's emissions have the following associated energy levels and emission intensities equal or over 1% [21]:

- 4761.0 keV: 1.00%;
- 4797.8 keV: 1.50%;
- 4814.6 keV: 9.30%;
- 4838.0 keV: 5.00%;
- 4845.3 keV: 56.20%;
- 4901.0 keV: 10.20%;
- 4967.5 keV: 5.97%;
- 4978.5 keV: 3.17%;
- 5053.0 keV: 6.60%.

Knowing this information and forcing equal shape factors, it is possible to drastically reduce the variables involved from 36 to 5:

- One activity variable (A) is sufficient to calculate the rest via intensity proportions.
- σ and τ only need one variable each, since they are going to be the assumed equal for the rest.

- For the μ parameter, as the measurement is found displaced (and nonlinearly so), it is necessary to set a reference value for the displacement and a proportion of the theoretical energy differences.

Although the energy shift is not linear, the emissions take place in a close enough range (<350 keV) to make a linear behavior assumption possible. The result is shown in Figure 9, where the overlapped spectrum of Th-230 and Th-229 can be observed.

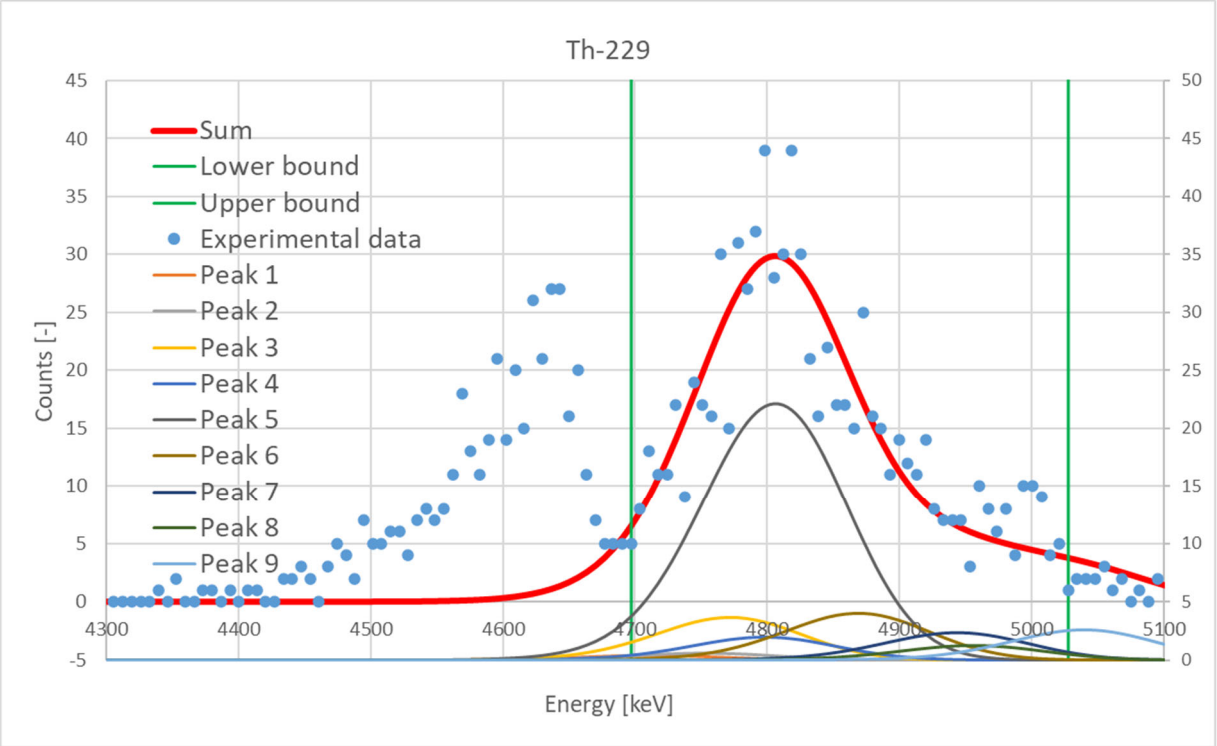


Figure 9. Thorium spectrometry: Th-229 approximation using nine erfc-based distributions of Th-229 emission data with the following simplified parameters: energy, displacement and shape factors.

The approximation of the Th-229 spectrum has been performed with nine erf distributions using the aforementioned Th-229 emission data. The approximation region is restricted by lower and upper bounds.

Now, it is possible to perform the same procedure as we did with uranium, always bearing in mind that less than a 3% error has an influence on the uncertainty of the results (Table 11).

Table 11. Result of the Th-229 spectrometry approximation, with energy, displacement and shape factor simplifications.

Study Region	Channel [-]	Energy [keV]	Experimental Counts [-]	Estimated Counts [-]	Count Difference [-]	Error [%]
Undisturbed Th-229	366 415	4697.13 5027.84	760	738.64	−21.36	−2.811

4. Conclusions

The use of the Evolutionary method to fit the complementary error function to experimental spectra provides congruent results and is an adequate tool for deconvoluting peaks obtained from TENORM samples, which permits diminishing the time and resources

needed to properly determine its activity concentration. The good agreement between the tracer's experimental spectra and the fitted ones has allowed the authors to apply it to such a complex variety of samples as TENORM industries' by-product samples. In this work, samples of extracted water from gas extraction, uranium mining and thorium fabrics have been used. The used algorithm allows the analyst in charge to adjust the fitting parameters to the experimental spectrum, providing the ability to adapt to the great degree of variability that experimental spectra shows and to evaluate the activity of the samples despite the presence of overlaps.

The goodness of each approximation is established when the following conditions are achieved: the error associated to the fitting should be lower than that associated with the analyst's work (5%) and the shape factors cannot differ by more than 20%.

Author Contributions: Conceptualization, C.O.; methodology, C.O., A.G. and M.H.; algorithm, A.G.; investigation, all authors.; writing—original draft preparation, C.O.; writing—review and editing, C.O. and A.G. All authors have read and agreed to the published version of the manuscript.

Funding: This research received no external funding, but the authors acknowledge funding from SENyRAD (IT1694-22), a research group at the Basque University System of the Basque Government (Spain). Open Access funding was partially provided by the University of Basque Country.

Data Availability Statement: The original contributions presented in the study are included in the article; further inquiries can be directed to the corresponding author.

Conflicts of Interest: The authors declare no conflicts of interest.

Abbreviations

The following abbreviations are used in this manuscript:

ROI	Region of Interest
LSM	Least Squared Mean

References

1. US EPA. Technologically Enhanced Naturally Occurring Radioactive Materials (TENORM). Updated 2014. Available online: https://www.epa.gov/radiation/technologically-enhanced-naturally-occurring-radioactive-materials-tenorm (accessed on 23 December 2025).
2. Al Nabhani, K.; Khan, F. The importance of public participation in legislation of TENORM risks management in the oil and gas industry. In *Nuclear Radioactive Materials in the Oil and Gas Industry*; Elsevier: Amsterdam, The Netherlands, 2020; pp. 229–257. [CrossRef]
3. Sahoo, P.; Joseph, J. Radioactive hazards in utilization of industrial by-products: Comprehensive review. *J. Hazard. Toxic Radioact. Waste* **2021**, *25*, 03121001. [CrossRef]
4. Pommé, S. Typical uncertainties in alpha-particle spectrometry. *Metrologia* **2014**, *52*, S146–S155. [CrossRef]
5. L'Annunziata, M.F. *Handbook of Radioactivity Analysis*, 3rd ed; Academic Press: Amsterdam, The Netherlands, 2012. Available online: https://www.sciencedirect.com/book/edited-volume/9780123848734/handbook-of-radioactivity-analysis (accessed on 22 January 2026).
6. Olondo, C.; Idoeta, R.; Herranz, M. Alpha spectrometry: Avoiding recoil contamination of solid state alpha detectors. *Nucl. Eng. Technol.* **2024**, *56*, 4661. [CrossRef]
7. Díaz-Francés, J.A.; Cortés-Giraldo, M.A.; Jiménez-Ramos, M.C.; Hurtado-Bermúdez, S. Simulation of the response of a PIPS detector using GEANT4 code. *Nucl. Instrum. Methods Phys. Res. Sect. A Accel. Spectrometers Detect. Assoc. Equip.* **2017**, *875*, 21–26. [CrossRef]
8. Trivedi, B.M.P. *Least Squares Analysis of Experimental Alpha Spectra*; Carnegie-Mellon University: Pittsburg, PA, USA, 1969; pp. 97–104.
9. Baba, H. A computer program for α spectrum analysis. *Nucl. Instrum. Methods* **1978**, *148*, 173–178. [CrossRef]
10. Wätzig, W.; Westmeier, W. Alfun—A program for the evaluation of complex alpha-spectra. *Nucl. Instrum. Methods* **1978**, *153*, 517–524. [CrossRef]

11. García-Toraño, E.; Aceña, M.L. Nolin: Nonlinear analysis of complex alpha spectra. *Nucl. Instrum. Methods Phys. Res.* **1981**, *185*, 261–269. [CrossRef]
12. L'hoir, A. Study of the asymmetrical response of silicon surface barrier detectors to MeV light ions. Application to the precise analysis of light ions energy spectra I. helium ions. *Nucl. Instrum. Methods Phys. Res.* **1984**, *223*, 336–345. [CrossRef]
13. Bortels, G.; Collaers, P. Analytical function for fitting peaks in alpha-particle spectra from si detectors. *Appl. Radiat. Isot.* **1987**, *38*, 831–837. [CrossRef]
14. Steinbauer, E.; Bortels, G.; Bauer, P.; Biersack, J.P.; Burger, P.; Ahmad, I. A survey of the physical processes which determine the response function of silicon detectors to alpha particles. *Nucl. Instrum. Methods Phys. Res. Sect. A Accel. Spectrometers Detect. Assoc. Equip.* **1994**, *339*, 102–108. [CrossRef]
15. Pöllänen, R.; Siiskonen, T. Unfolding alpha-particle energy spectrum from a membrane air filter containing radon progeny. *Radiat. Meas.* **2014**, *70*, 15–20. [CrossRef]
16. Pommé, S.; Caro Marroyo, B. Improved peak shape fitting in alpha spectra. *Appl. Radiat. Isot.* **2014**, *96*, 148. [CrossRef] [PubMed]
17. Siiskonen, T.; Pöllänen, R. New approach to spectrum analysis-iterative monte carlo simulations and fitting. *Prog. Nucl. Sci. Technol.* **2011**, *2*, 437–441. [CrossRef]
18. Westmeier, W.; Siemon, K. A paradigm shift in nuclear spectrum analysis. *IEEE Trans. Nucl. Sci.* **2012**, *59*, 1296–1299. [CrossRef]
19. Yan, Q.; Zhang, H.; Huang, J.; Xiong, W.; Huang, G.; Dai, L.; Wu, Z.; Liu, G. Quantitative alpha spectra isotope identification based on deep learning method and monte carlo modeling. *Radiat. Meas.* **2025**, *186*, 107460. [CrossRef]
20. Baeza, A.; Miranda, J.; Guillén, J.; Corbacho, J.A.; Pérez, R. A new approach to the analysis of alpha spectra based on neural network techniques. *Nucl. Instrum. Methods Phys. Res. Sect. A Accel. Spectrometers Detect. Assoc. Equip.* **2011**, *652*, 450–453. [CrossRef]
21. Firestone, R.; Browne, E. *Table of Radioactive Isotopes*; John Wiley and Sons: Hoboken, NJ, USA, 1986.

Disclaimer/Publisher's Note: The statements, opinions and data contained in all publications are solely those of the individual author(s) and contributor(s) and not of MDPI and/or the editor(s). MDPI and/or the editor(s) disclaim responsibility for any injury to people or property resulting from any ideas, methods, instructions or products referred to in the content.